

## Suppression of weak antilocalization in $\text{Ga}_x\text{In}_{1-x}\text{As}/\text{InP}$ narrow quantum wires

Th. Schäpers,<sup>1</sup> V. A. Guzenko,<sup>1</sup> M. G. Pala,<sup>2</sup> U. Zülicke,<sup>3</sup> M. Governale,<sup>4</sup> J. Knobbe,<sup>1</sup> and H. Hardtdegen<sup>1</sup>

<sup>1</sup>*Institute for Bio- and Nanosystems (IBN-1) and Virtual Institute of Spin Electronics (VISEL), Research Centre Jülich GmbH, 52425 Jülich, Germany*

<sup>2</sup>*IMEP-MINATEC (UMR CNRS-INPG-UJF 5130), 23 rue des Martyrs, Boîte Postale 257, 38016 Grenoble, France*

<sup>3</sup>*Institute of Fundamental Sciences and MacDiarmid Institute for Advanced Materials and Nanotechnology, Massey University, Private Bag 11 222, Palmerston North, New Zealand*

<sup>4</sup>*Institut für Theoretische Physik III, Ruhr-Universität Bochum, 44780 Bochum, Germany*

(Received 21 June 2006; published 2 August 2006)

The magnetoconductivity of  $\text{Ga}_x\text{In}_{1-x}\text{As}/\text{InP}$  quantum wires with widths in the range of 1220–250 nm was investigated. The finite zero-field spin splitting in our samples gives rise to spin relaxation and weak antilocalization in wide wires. In contrast, for the narrow wires, only weak-localization behavior is seen even though the zero-field spin splitting is independent of wire width. The observed renormalization of the spin-relaxation length due to purely geometrical effects can be described quantitatively using a model where the effect of spin precession is represented by spin-dependent pseudomagnetic fluxes, and by exact numerical transport calculations.

DOI: 10.1103/PhysRevB.74.081301

PACS number(s): 73.20.Fz, 73.63.Nm

Controlled spin precession in semiconductor heterostructures is a key mechanism in spin-electronic devices<sup>1</sup> where electric current is manipulated by addressing the electrons' spin instead of their charge. In two-dimensional electron gases (2DEGs) realized in III-V semiconductor heterostructures, spin-orbit coupling gives rise to a spin precession at zero external magnetic field. Possible origins of zero-field spin splitting can be the lack of inversion symmetry of the crystal lattice (bulk inversion asymmetry),<sup>2</sup> and the structural macroscopic electric field present in an asymmetric quantum well.<sup>3</sup> The latter is called Rashba spin-orbit coupling and can be controlled by external gate voltages,<sup>4–7</sup> which makes this mechanism especially interesting for spin-electronic devices.<sup>8</sup> A detailed understanding of spin-orbit effects in nanostructures and elucidation of methods for their accurate measurement is therefore of great current interest. Here we report on an experimental study of the interplay between spin precession and quantum interference in quasiballistic semiconductor nanowires, which complements previous studies performed in 2DEGs,<sup>9–16</sup> dirty quantum wires,<sup>17</sup> and ballistic quantum dots.<sup>18</sup> We observe a remarkable sign change of the quantum correction to the conductance, signifying a crossover from weak antilocalization (WAL) to weak localization (WL) as the wire width is reduced. Detailed experimental and theoretical investigations show that this effect arises from the confined orbital dynamics of electrons in narrow wires and not from a changed value of the Rashba spin splitting.

The measurement of the quantum correction to the conductance is a versatile tool to investigate spin-orbit coupling in 2DEGs. In a system with spin-rotational invariance (i.e., without spin-orbit coupling) and in the absence of external magnetic fields, contributions of time-reversed electron paths to the quantum-mechanical backscattering amplitude interfere coherently, leading to an increased resistance (WL) for a quantum-coherent conductor.<sup>19</sup> A finite spin-orbit coupling introduces random deviations between the spin states of electrons that are backscattered on time-reversed paths. The resulting spin-space average suppresses the quantum correc-

tion to the conductance and changes its sign (WAL).<sup>19,20</sup> Quantitative analysis of the magnetoconductance was used to extract the characteristic spin-relaxation time  $\tau_{so}$  in various types of heterostructures; e.g.,  $\text{AlGaAs}/\text{GaAs}$ ,<sup>10</sup>  $\text{GaInAs}/\text{AlInAs}$ ,<sup>13</sup>  $\text{GaInAs}/\text{InP}$ ,<sup>9,15</sup> and  $\text{AlSb}/\text{InAs}/\text{AlSb}$ .<sup>11</sup> For 2DEGs covered by a metal electrode<sup>13,14</sup> as well as for gated InAs nanowires,<sup>21</sup> it was confirmed by WAL measurements that  $\tau_{so}$  can be controlled by a gate voltage that effectively tunes the Rashba spin splitting. In contrast, we show in this Rapid Communication how wire confinement affects spin relaxation. Our measurements were performed on quantum wires fabricated in  $\text{GaInAs}/\text{InP}$  heterostructures, which are well known for showing a large Rashba spin splitting.<sup>22</sup> We start by describing the experimental method and presenting measured data. Our interpretation of the observed WAL-WL crossover as a confinement-induced effect is explained afterward, and results of supporting numerical simulations are shown.

The  $\text{Ga}_{0.47}\text{In}_{0.53}\text{As}/\text{Ga}_{0.23}\text{In}_{0.77}\text{As}/\text{InP}$  heterostructure was grown by metal-organic vapor-phase epitaxy on a semi-insulating InP substrate. The layer system is shown schematically in inset (a) of Fig. 2 below. Quantum-wire structures were defined using electron-beam lithography and reactive ion etching.<sup>7</sup> A number of 160 identical wires, each 620  $\mu\text{m}$  long, were connected in parallel. Six sets of wires were analyzed with a width ranging from 1220 nm down to 250 nm. An electron-beam micrograph of the 250 nm wide wires is shown in Fig. 1, inset (a). From magnetoresistance measurements in a reference Hall bar sample fabricated on the same chip, a carrier concentration of  $n=5.3 \times 10^{11} \text{ cm}^{-2}$  and a mobility of  $\mu=205\,000 \text{ cm}^2/\text{V s}$  at 0.6 K were determined. Analysis of the temperature-dependent Shubnikov–de Haas oscillations yielded an effective electron mass  $m^*=0.039m_e$ . A clear beating pattern exhibited in the Shubnikov–de Haas oscillations indicates the presence of Rashba spin-orbit coupling. We extracted a Rashba coupling parameter of  $\alpha_R=4.84 \times 10^{-12} \text{ eV m}$  from the  $1/B$  fast Fourier transform of the magnetoresistance.<sup>22</sup>

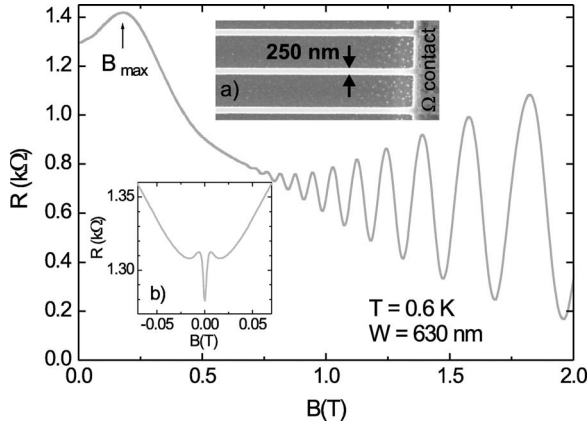


FIG. 1. Magnetoresistance of the 630-nm-wide set of wires at 0.6 K. Inset (a) shows a scanning electron micrograph of a detail of the 250-nm-wide set of wires with the Ohmic contact pads. In inset (b) a detail of the magnetoresistance close to  $B=0$  of the 630 nm wire is shown.

The magnetoresistance of the set of 630 nm wide wires over a larger field range is shown exemplarily in Fig. 1. Clear Shubnikov–de Haas oscillations were observed for magnetic fields above 0.5 T. The electron concentration extracted from the  $1/B$  fast Fourier transform is, as for all other sets of wires, identical to the one obtained from the Hall bar sample. A resistance maximum is found at  $B_{\max}=0.18$  T which can be attributed to diffusive boundary scattering. For decreasing widths of the wires this maximum shifts to higher magnetic fields. We use  $B_{\max}$  to calculate the electrical width of the quantum wires using the expression  $W_{\text{eff}} \approx 0.55 \hbar k_F / (eB_{\max})$ ,<sup>23</sup> where  $e$  is the elementary charge and  $k_F$  the Fermi wave number. The values of  $W_{\text{eff}}$  for all wires are summarized in Table I.

The conductivity  $\sigma$  and the mobility  $\mu$  were determined for each set of wires using  $W_{\text{eff}}$  as the width of conducting area. As seen in Fig. 1 inset (b), a sharp dip appears in the magnetoresistance at  $B=0$  for the 630-nm-wide wire which can be attributed to WAL. The transition to a decreasing resistance with increasing magnetic field at  $\approx 7$  mT is due to

TABLE I. Summary of values for relevant length and time scales in our samples. The geometrical wire width  $W$ , effective electrical wire width  $W_{\text{eff}}$ , elastic scattering time  $\tau_{\text{el}}$ , elastic mean free path  $l_{\text{el}}$ , phase coherence time  $\tau_{\phi}$ , and phase coherence length  $l_{\phi}$  are extracted from transport data.  $l_{\text{so}}^{(\text{est})}$  is an estimate for the spin-relaxation length according to Eq. (1).

$W$ (nm)	$W_{\text{eff}}$ (nm)	$\tau_{\text{el}}$ (ps)	$l_{\text{el}}$ ( $\mu\text{m}$ )	$\tau_{\phi}$ at 0.6 K (ps)	$l_{\phi}$ at 0.6 K ( $\mu\text{m}$ )	$l_{\text{so}}^{(\text{est})}$ ( $\mu\text{m}$ )
1220	1180	4.47	2.42	103.79	8.25	0.5
1020	830	4.33	2.35	83.60	7.29	0.7
830	570	3.56	1.93	62.73	5.72	0.9
630	410	2.41	1.30	45.26	4.00	0.9
340	210	1.14	0.62	23.24	1.97	1.1
250	120	0.79	0.43	14.35	1.29	1.8

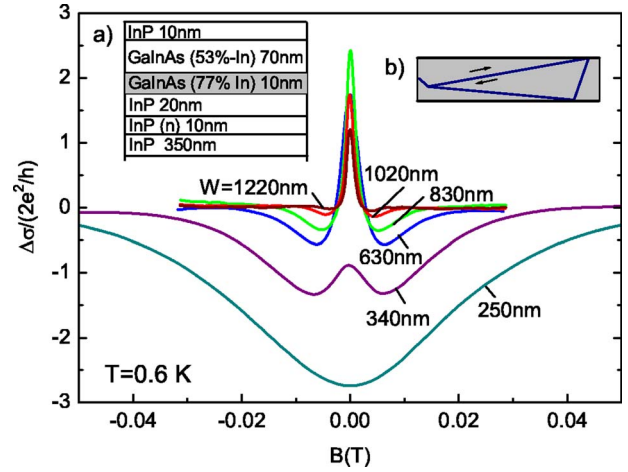


FIG. 2. (Color online) Magnetoconductivity corrections  $\Delta\sigma$  in units of  $2e^2/h$  for various wire widths  $W$  at a temperature of 0.6 K. The layer sequence of the heterostructures is shown in inset (a). The inset (b) shows a typical loop for a narrow wire.

weak localization being the dominant contribution at higher fields.

Data shown in Fig. 2 illustrate how WAL observed for wider wires is suppressed for narrow wires. In contrast to the previous figure, the quantum correction  $\Delta\sigma$  to the two-dimensional conductivity is plotted in units of  $2e^2/h$ . The occurrence of WAL is thus indicated by an enhanced conductivity at  $B=0$ .<sup>36</sup> The decrease of peak height as the wire width is reduced from 1220 to 830 nm reflects the expected  $1/W_{\text{eff}}$  scaling of the quantum correction to the 2D conductivity.<sup>24</sup> Simultaneously the minimum in  $\Delta\sigma$  indicating the transition to WL is shifted toward larger magnetic fields. As the wire width is reduced further, the WAL peak starts to decrease and completely vanishes for the narrowest wire of 250 nm width. Thus only WL is observed for the very narrow wires.

To understand the apparent suppression of WAL, we analyzed the relative values of spin-relaxation length  $l_{\text{so}} = \sqrt{D\tau_{\text{so}}}$ , elastic mean free path  $l_{\text{el}}$ , and phase-coherence length  $l_{\phi}$ . Here,  $D$  denotes the diffusion constant. Fundamentally, spin relaxation in our wires arises due to the spin precession that is induced by the presence of Rashba spin splitting. In our samples, it was found that the Rashba coupling parameter  $\alpha_R$  does not depend on the wire width.<sup>25</sup> Hence, the ballistic spin-precession length  $l_R = \hbar^2 / (2m^* \alpha_R)$  is identical for all wires and given by  $l_R = 200$  nm. In the 2D limit,<sup>26</sup>  $l_{\text{so}} = l_R$ , but the observed WAL-WL crossover indicates that  $l_{\text{so}}$  in wires must have a strong width dependence. Intuitively, we expect a suppression of spin relaxation in ballistic narrow wires, as the elongated shape of relevant closed paths [see Fig. 2 inset (b)] effectively reduces the magnitude of accumulated random spin phases. A more quantitative analysis is possible using the concept of spin-orbit-induced effective magnetic fluxes.<sup>14,27</sup> In complete analogy with the width dependence of the magnetic dephasing length in wires,<sup>24</sup> we find an estimate

$$l_{\text{so}}^{(\text{est})} = \begin{cases} \frac{\sqrt{3}l_{\text{R}}^2}{W_{\text{eff}}} & \text{for } l_{\text{el}} < W_{\text{eff}}, \\ l_{\text{R}} \sqrt{\frac{C_1 l_{\text{el}} l_{\text{R}}^2}{2 W_{\text{eff}}^3} + \frac{C_2 l_{\text{el}}^2}{2 W_{\text{eff}}^2}} & \text{for } l_{\text{el}} > W_{\text{eff}}. \end{cases} \quad (1)$$

The constants  $C_1$  and  $C_2$  depend on the type of boundary scattering (specular or diffusive) in the wire.<sup>24</sup> As will be seen from the discussion presented in the following paragraph, our wires are in the regime where  $l_{\text{el}} > W_{\text{eff}}$ .

The elastic scattering times  $\tau_{\text{el}} = \mu m^* / e$  as well as the corresponding elastic mean free path  $l_{\text{el}} = v_{\text{F}} \tau_{\text{el}}$  were extracted from the mobility and the electron concentration of the wires (see Table I).<sup>37</sup> The observed decrease of  $l_{\text{el}}$  for reduced wire widths can be explained by the additional contribution of diffusive boundary scattering. In contrast to the case of total specular boundary scattering where the conductivity of the wires remains equal to the conductivity of the 2DEG, presence of the diffusive boundary scattering leads to its reduction. For the narrowest set of wires a probability  $p$  of specular boundary scattering of 0.5 was estimated following the approach described in Ref. 28. The large contribution of diffusive boundary scattering can be attributed to the relatively rough boundaries resulting from definition of the wires by reactive ion etching. A comparison of the elastic mean free path  $l_{\text{el}}$  with the spin-precession length  $l_{\text{R}}$  reveals that, owing to the strong Rashba effect in our structures, the value of  $l_{\text{R}}$  is always shorter than the mean distance between two scattering centers. Furthermore, all of our wires are in the quasiballistic regime where  $l_{\text{el}} > W_{\text{eff}}$ .

In our case the inelastic scattering time  $\tau_{\phi}$  cannot be extracted directly from the experiment, however it can be reliably estimated<sup>28</sup> by the following expression:<sup>29</sup>

$$\frac{1}{\tau_{\phi}} = \frac{\pi (k_{\text{B}} T)^2}{2 \hbar E_{\text{F}}} \ln \left( \frac{E_{\text{F}}}{k_{\text{B}} T} \right) + \left( \frac{\pi k_{\text{B}} T}{\sqrt{D} W_{\text{eff}} m^*} \right)^{2/3}, \quad (2)$$

with  $E_{\text{F}}$  being the Fermi energy. The inelastic mean free path is given by  $l_{\phi} = \sqrt{D} \tau_{\phi}$ . As can be seen in Table I,  $l_{\phi}$  at 0.6 K is reduced from 8.25  $\mu\text{m}$  for the 1220-nm-wide wires to 1.29  $\mu\text{m}$  for the narrowest ones. Nevertheless,  $l_{\phi}$  at this temperature exceeds the elastic mean free path  $l_{\text{el}}$  as well as the spin-precession length  $l_{\text{R}}$  for all wires.

Suppression of weak antilocalization occurs when the spin-relaxation length  $l_{\text{so}}$  exceeds the phase-coherence length  $l_{\phi}$ , because no significant spin-dependent phases can be accumulated then by coherently backscattered electrons. We can estimate  $l_{\text{so}}$  according to Eq. (1) for each wire and compare these with the extracted value of  $l_{\phi}$  in the same system. (See Table I. We have used the values of  $C_{1,2}$  for diffusive boundary scattering.<sup>24</sup>) The conspicuously large value found for  $l_{\text{so}}^{(\text{est})}$  in the narrowest wire is consistent with the observed absence of WAL in its magnetoconductance. For all the other wires,  $l_{\text{so}}^{(\text{est})} < l_{\phi}$ , and signatures of WAL are seen in the transport data (see Fig. 2). Temperature-dependent measurements displayed in Fig. 3 provide further support for this explanation. At the lowest temperature, a signature of WAL is superimposed on a negative (i.e., localizing) correction to the conductance. As temperature is increased, the WAL peak gets

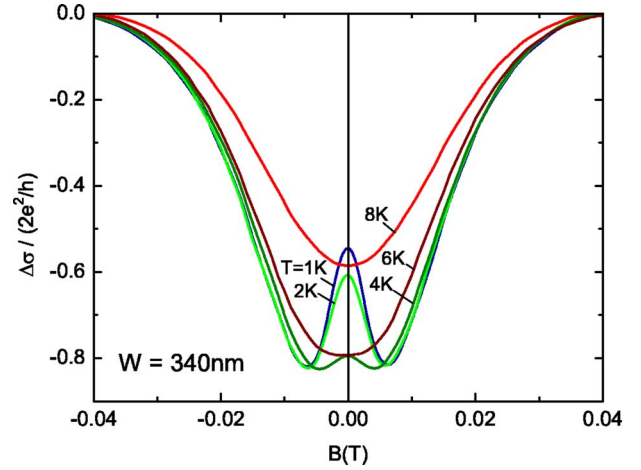


FIG. 3. (Color online) Magnetoconductance corrections of the set of 340-nm-wide wires for temperatures from 1 to 8 K.

progressively weaker until, for temperatures above 6 K, any trace of WAL has vanished. Evidently, the decrease of  $l_{\phi}$  below the spin-relaxation length renders spin effects irrelevant, obliterating the WAL signal. At the crossover temperature of 4 K, we obtain a phase-coherence length of 0.94  $\mu\text{m}$ , which agrees quite well with the spin-relaxation length estimated from Eq. (1) and given in Table I.

It appears that modeling spin precession by spin-dependent fluxes<sup>14,27</sup> yields a quantitative agreement with the observed WAL-WL crossover in our wires. However, further analysis is needed to confirm this result, because the approach yielding Eq. (1) neglects the non-Abelian nature of spin-dependent gauge fields that are associated with spin-orbit coupling. Additional spin relaxation arising from non-Abelian contributions can be expected to become relevant in the limit  $l_{\text{R}} < \sqrt{W_{\text{eff}} l_{\text{el}}}$ . To make sure that non-Abelian contributions do not destroy, in principle, the effective renormal-

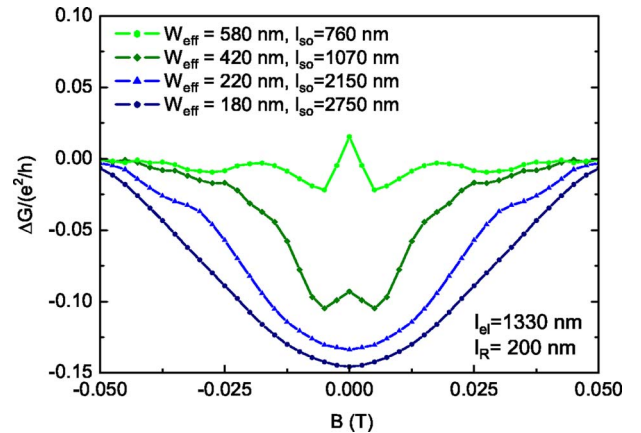


FIG. 4. (Color online) Quantum correction to the magnetoconductance, calculated for disordered wires with length  $L = 2 \mu\text{m}$ , Rashba coefficient  $\alpha_{\text{R}} = 4.8 \times 10^{-12} \text{ eV m}$ , and mean free path  $l_{\text{el}} = 1.33 \mu\text{m}$ . From top to bottom, curves correspond to  $W_{\text{eff}} = 580, 420, 220, 180 \text{ nm}$ . Indicated values for  $l_{\text{so}}$  were estimated using Eq. (1). Conductances were obtained by averaging over 50 different configurations of random bulk impurities and 50 slightly different energy values.

ization of spin relaxation in our narrow wires, we performed numerical transport calculations where the effect of spin-orbit coupling is treated exactly. A spin-dependent tight-binding model is adopted to describe a quasi-1D wire with finite Rashba spin splitting.<sup>30</sup> The total zero-temperature Green's function of the system is calculated using a recursive method,<sup>31,32</sup> and the quantum-mechanical transmission and reflection coefficients are found using a standard procedure.<sup>33</sup> These yield the conductance by means of the Landauer-Büttiker formula,<sup>34,35</sup> from which the quantum correction is extracted. We assume that the external leads that are attached to our system are subject to the same homogeneous magnetic field as is present in the sample, but have no spin-orbit coupling. In Fig. 4, we show quantum corrections to the magnetoconductance for a set of wires with different widths, all having the same Rashba spin-splitting parameter  $\alpha_R$ . Mirroring the experimental observation, WAL behavior is exhibited in the simulations for large  $W_{\text{eff}}$ , but is suppressed for narrow wires. We calculated  $l_{\text{so}}^{(\text{est})}$  for the simu-

lated wires and, as for the experimental data, find WAL suppression whenever  $l_{\text{so}}^{(\text{est})}$  exceeds the wire length  $L$  (which plays the role of dephasing length  $l_\phi$  in our zero-temperature simulations). The striking congruence between experimental and numerical results, as well as the applicability of our analytical description in both cases, provide strong support for our interpretation of the WAL-to-WL crossover as a geometrical effect.

In conclusion, the effect of spin-orbit coupling on the quantum correction to the conductivity of GaInAs/InP wires was investigated. Although the bare spin splitting was the same in all wires, we observed a clear width dependence of spin relaxation. Wide wires showed WAL behavior, but only WL was found for very narrow wires. This WAL-WL crossover can be explained as being due to a confinement-induced suppression of spin relaxation as the wire width is decreased.

U.Z. is supported by the RSNZ Marsden Fund.

- <sup>1</sup>S. A. Wolf *et al.*, *Science* **294**, 1488 (2001).
- <sup>2</sup>G. Dresselhaus, *Phys. Rev.* **100**, 580 (1955).
- <sup>3</sup>Y. Bychkov and E. I. Rashba, *J. Phys. C* **17**, 6039 (1984).
- <sup>4</sup>J. Nitta, T. Akazaki, H. Takayanagi, and T. Enoki, *Phys. Rev. Lett.* **78**, 1335 (1997).
- <sup>5</sup>G. Engels, J. Lange, Th. Schäpers, and H. Lüth, *Phys. Rev. B* **55**, R1958 (1997).
- <sup>6</sup>Y. Sato, S. Gozu, T. Kikutani, and S. Yamada, *Physica B* **272**, 114 (1999).
- <sup>7</sup>Th. Schäpers, J. Knobbe, and V. A. Guzenko, *Phys. Rev. B* **69**, 235323 (2004).
- <sup>8</sup>S. Datta and B. Das, *Appl. Phys. Lett.* **56**, 665 (1990); J. Nitta, F. E. Meijer, and H. Takayanagi, *ibid.* **75**, 695 (1999); A. A. Kiselev and K. W. Kim, *ibid.* **78**, 775 (2001); M. Governale, D. Boese, U. Zülicke, and C. Schroll, *Phys. Rev. B* **65**, 140403(R) (2002).
- <sup>9</sup>Z. I. Alverov A. T. Gorelenok, V. V. Mamutin, T. A. Polyanskaya, I. G. Savel'ev, and Y. V. Shmartsev, *Sov. Phys. Semicond.* **18**, 1247 (1984).
- <sup>10</sup>P. D. Dresselhaus, C. M. A. Papavassiliou, R. G. Wheeler, and R. N. Sacks, *Phys. Rev. Lett.* **68**, 106 (1992).
- <sup>11</sup>G. L. Chen, J. Han, T. T. Huang, S. Datta, and D. B. Janes, *Phys. Rev. B* **47**, 4084 (1993).
- <sup>12</sup>W. Knap *et al.*, *Phys. Rev. B* **53**, 3912 (1996).
- <sup>13</sup>T. Koga, J. Nitta, T. Akazaki, and H. Takayanagi, *Phys. Rev. Lett.* **89**, 046801 (2002).
- <sup>14</sup>J. B. Miller, D. M. Zumbühl, C. M. Marcus, Y. B. Lyanda-Geller, D. Goldhaber-Gordon, K. Campman, and A. C. Gossard, *Phys. Rev. Lett.* **90**, 076807 (2003).
- <sup>15</sup>S. A. Studenikin, P. T. Coleridge, N. Ahmed, P. J. Poole, and A. Sachrajda, *Phys. Rev. B* **68**, 035317 (2003).
- <sup>16</sup>F. E. Meijer, A. F. Morpurgo, T. M. Klapwijk, and J. Nitta, *Phys. Rev. Lett.* **94**, 186805 (2005).
- <sup>17</sup>C. Kurdak, A. M. Chang, A. Chin, and T. Y. Chang, *Phys. Rev. B* **46**, 6846 (1992).
- <sup>18</sup>D. M. Zumbühl, J. B. Miller, C. M. Marcus, K. Campman, and A. C. Gossard, *Phys. Rev. Lett.* **89**, 276803 (2002).
- <sup>19</sup>G. Bergmann, *Phys. Rep.* **107**, 1 (1984).
- <sup>20</sup>S. Hikami, A. I. Larkin, and Y. Nagaoka, *Prog. Theor. Phys.* **63**, 707 (1980).
- <sup>21</sup>A. E. Hansen, M. T. Björk, I. C. Fath, C. Thelander, and L. Samuelson, *Phys. Rev. B* **71**, 205328 (2005).
- <sup>22</sup>Th. Schäpers G. Engels, J. Lange, Th. Klocke, M. Hollfelder, and H. Lüth, *J. Appl. Phys.* **83**, 4324 (1998).
- <sup>23</sup>T. J. Thornton, M. L. Roukes, A. Scherer, and B. P. Van de Gaag, *Phys. Rev. Lett.* **63**, 2128 (1989).
- <sup>24</sup>C. W. J. Beenakker and H. van Houten, *Phys. Rev. B* **38**, 3232 (1988).
- <sup>25</sup>V. A. Guzenko, J. Knobbe, H. Hardtdegen, Th. Schäpers, and A. Bringer, *Appl. Phys. Lett.* **88**, 032102 (2006).
- <sup>26</sup>S. V. Iordanskii, Y. B. Lyanda-Geller, and G. E. Pikus, *JETP Lett.* **60**, 206 (1994).
- <sup>27</sup>I. L. Aleiner and V. I. Fal'ko, *Phys. Rev. Lett.* **87**, 256801 (2001).
- <sup>28</sup>J. A. Katine, M. J. Berry, R. M. Westervelt, and A. C. Gossard, *Phys. Rev. B* **57**, 1698 (1998).
- <sup>29</sup>B. L. Al'tshuler, A. G. Aronov, and D. E. Khmel'nitsky, *J. Phys. C* **15**, 7367 (1982).
- <sup>30</sup>M. G. Pala, M. Governale, U. Zülicke, and G. Iannaccone, *Phys. Rev. B* **71**, 115306 (2005).
- <sup>31</sup>H. U. Baranger, D. P. DiVincenzo, R. A. Jalabert, and A. D. Stone, *Phys. Rev. B* **44**, 10637 (1991).
- <sup>32</sup>D. Frustaglia, M. Hentschel, and K. Richter, *Phys. Rev. Lett.* **87**, 256602 (2001).
- <sup>33</sup>D. S. Fisher and P. A. Lee, *Phys. Rev. B* **23**, 6851 (1981).
- <sup>34</sup>R. Landauer, *IBM J. Res. Dev.* **1**, 223 (1957).
- <sup>35</sup>M. Büttiker, *Phys. Rev. Lett.* **57**, 1761 (1986).
- <sup>36</sup>We determined the quantum correction to the resistance by subtracting the classical (Drude) contribution. The latter was found from a fit to a  $B^2$  field dependence.
- <sup>37</sup>As our measurements were performed in a two-terminal configuration, a contact resistance of 270  $\Omega$  was subtracted before calculating the specific conductance.